



Surface energy exchanges along a tundra-forest transition and feedbacks to climate

Jason Beringer^{a,*}, F. Stuart Chapin III^b, Catharine C. Thompson^b,
A. David McGuire^c

^a School of Geography and Environmental Science, P.O. Box 11A, Monash University, Clayton, Vic. 3800, Australia

^b Institute of Arctic Biology, University of Alaska Fairbanks, Fairbanks, AK 99775, USA

^c U.S. Geological Survey, Alaska Cooperative Fish and Wildlife Research Unit,
University of Alaska Fairbanks, Fairbanks, AK 99775, USA

Received 21 October 2004; accepted 17 May 2005

Abstract

Surface energy exchanges were measured in a sequence of five sites representing the major vegetation types in the transition from arctic tundra to forest. This is the major transition in vegetation structure in northern high latitudes. We examined the influence of vegetation structure on the rates of sensible heating and evapotranspiration to assess the potential feedbacks to climate if high-latitude warming were to change the distribution of these vegetation types. Measurements were made at Council on the Seward Peninsula, Alaska, at representative tundra, low shrub, tall shrub, woodland (treeline), and boreal forest sites. Structural differences across the transition from tundra to forest included an increase in the leaf area index (LAI) from 0.52 to 2.76, an increase in canopy height from 0.1 to 6.1 m, and a general increase in canopy complexity. These changes in vegetation structure resulted in a decrease in albedo from 0.19 to 0.10 as well as changes to the partitioning of energy at the surface. Bulk surface resistance to water vapor flux remained virtually constant across sites, apparently because the combined soil and moss evaporation decreased while transpiration increased along the transect from tundra to forest. In general, sites became relatively warmer and drier along the transect with the convective fluxes being increasingly dominated by sensible heating, as evident by an increasing Bowen ratio from 0.94 to 1.22. The difference in growing season average daily sensible heating between tundra and forest was 21 W m^{-2} . Fluxes changed non-linearly along the transition, with both shrubs and trees substantially enhancing heat transfer to the atmosphere. These changes in vegetation structure that increase sensible heating could feed back to enhance warming at local to regional scales. The magnitude of these vegetation effects on potential high-latitude warming is two to three times greater than suggested by previous modeling studies.

© 2005 Elsevier B.V. All rights reserved.

Keywords: Arctic; Surface energy exchanges; Eddy covariance; Biotic feedbacks; Treeline; Climate change

* Corresponding author. Tel.: +61 3 9905 9352; fax: +61 3 9905 2948.

E-mail address: Jason.beringer@arts.monash.edu.au (J. Beringer).

1. Introduction

High-latitude ecosystems play an important role in the functioning of the earth system because they occupy a large area, are sensitive to changes in climate, influence the exchange of water, energy, and radiatively active gases with the atmosphere, and affect local-regional (McFadden et al., 1998; Chapin et al., 2000b) and global climate (Bonan et al., 1992; Ciais et al., 1995; Foley et al., 1994). Functional responses of arctic tundra to changes in climate could influence global climate through both direct impacts on the radiation and energy balance and the exchange of radiatively active gases with the atmosphere (Bonan et al., 1995; McGuire et al., 2000; Reeburgh and Whalen, 1992). Some of the most important of these functional responses may involve changes in the composition and distribution of vegetation (Kittel et al., 2000; Levis et al., 1999).

Both modeling and observational studies provide evidence of changes in arctic vegetation distributions with increased air temperatures. Modeling studies suggest that enhanced warming would cause a northward shift of boreal woodland and forest (Kittel et al., 2000; Starfield and Chapin, 1996), resulting in a structural change from moist tussock tundra, which is dominated by tussock-forming sedges, to forest, which is dominated by trees (Walker et al., 1995). Shrub tundra, dominated by woody shrubs is an important structural intermediate between moist tussock tundra and forest. An increase in the abundance of shrubs with warming is suggested by field warming experiments over 10 years (Bret-Harte et al., 2001; Chapin et al., 1995; Hobbie et al., 1999), satellite-based studies of vegetation change over 30 years (Silapaswan, 2000), repeat aerial photography over 50 years (Sturm et al., 2001) and indigenous observations across the North American Arctic (Nickels et al., 2002; Thorpe et al., 2002). Paleovegetation studies also suggest that past-warming events caused a northward movement of shrubs and trees (MacDonald et al., 2000).

Such climatically induced shifts in vegetation types may amplify or reduce the effects of potential climatic change (Eugster et al., 2000). Modeling results indicate that a change from tussock tundra to shrub tundra could result in approximately a 3.4 W m^{-2} increase in summertime sensible heat flux, which is similar to the radiative forcing of 4.4 W m^{-2} that is the predicted effect of a doubling of atmospheric CO_2

concentration (Chapin et al., 2000b). It should be noted that the increase in summertime sensible heat is a local effect that depends on the extent of vegetation change, whereas changing atmospheric CO_2 concentrations occurs worldwide and therefore has a global effect. In an extensive comparison of observational and modeled feedbacks, Eugster et al. (2000) suggest that, under future warming, a vegetation change from tundra to shrub or shrub to forest would cause a positive feedback to atmospheric temperature but a negative feedback to atmospheric water vapor. The negative feedback to atmospheric water occurs because forests have a lower evapotranspiration rate that transfers less water vapor to the atmosphere (Eugster et al., 2000). Because water vapor is a strong greenhouse gas, the enhanced warming effect of the vegetation change is reduced.

Changes in the land-surface properties associated with canopy complexity may substantially alter water and energy exchange in transitional regions of arctic and boreal vegetation and may feed back to influence regional climate (Eugster et al., 2000). In order to address these potential feedbacks, we initiated a series of surface energy exchange measurements over the major high-latitude vegetation types along a gradient from tundra to forest. We measured key structural and micrometeorological properties of vegetation along this gradient, including leaf area, canopy height, bulk surface resistance and aerodynamic resistance. We also consider the canopy complexity, defined here as increasing height, biomass, and more intricate structure that results in multiple scattering and absorption of solar radiation and a concomitant decrease in albedo. This study is the first comparison of surface energy exchanges of the major high-latitude vegetation types measured in a single growing season under similar climatic conditions, allowing us to directly test the effects of vegetation structure on surface energy exchange, without the confounding effects of climatic differences.

2. Materials and methods

2.1. The Seward peninsula area and council

Data were collected at Council on the Seward Peninsula, located approximately 100 km northeast of

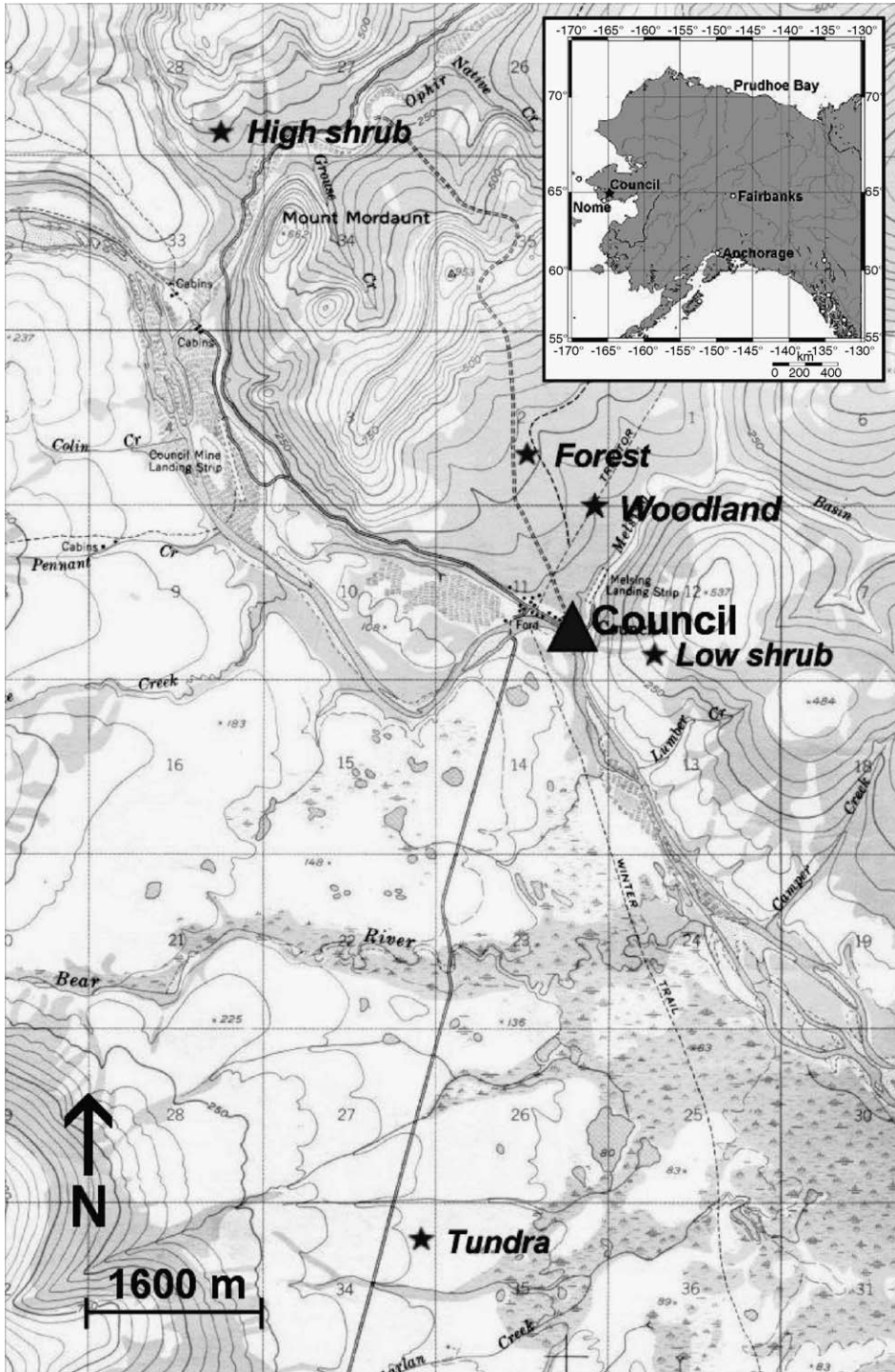


Fig. 1. Map of Alaska showing the Seward Peninsula and location of Council ($64^{\circ}50.499'N$ $163^{\circ}41.591'W$).

Nome, Alaska (Fig. 1). The Seward Peninsula in western Alaska was selected for study because there is a relatively smooth transition from forest to tundra, in contrast to the abrupt transition between forest and tundra in northern Alaska associated with the east–west trending Brooks Range. Monthly mean air temperatures in Nome range from -15°C in January to 11°C in July (mean 1950–1999) (Western Regional Climate Center). Average annual precipitation is 406 mm, including ~ 170 mm of snow water equivalent (1549 mm depth). Although long-term climate records do not exist for Council, the summer climate at Council during our study was warmer and drier

than at Nome, due to its more continental location. Because of the diversity of ecosystem types located in proximity to one another under the same climate regime, the Council area provided an excellent field site in which to investigate a variety of high-latitude ecosystem types that may be important in future climate change. In addition, the climate of the Peninsula is slightly wetter and warmer than the North Slope of Alaska because of the maritime influence (Fleming et al., 2000), allowing us to examine vegetation–climate feedbacks under a climate regime in which the expansion of forest to tundra is most likely to occur.

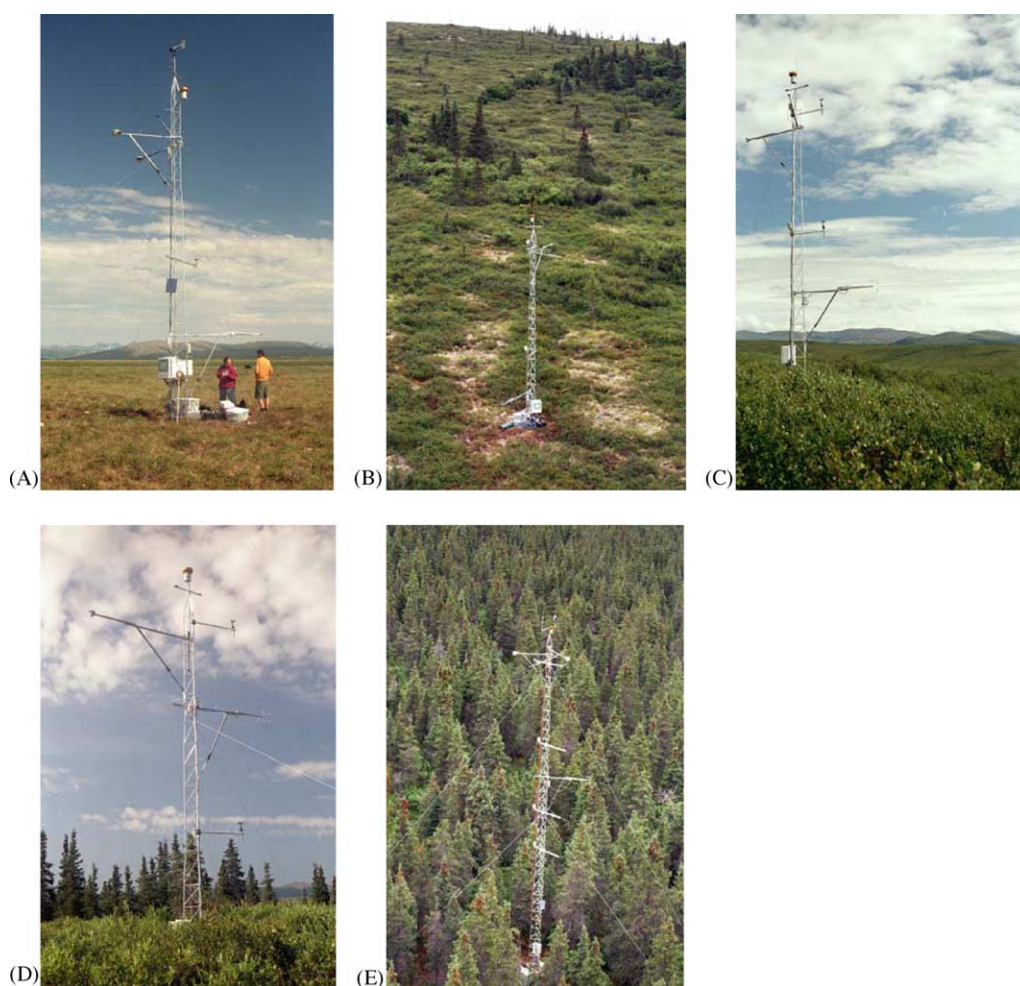


Fig. 2. The sites at Council along the vegetation gradient from tundra to forest. (A) Lichen dominated moist tussock tundra; (B) low shrub tundra; (C) tall shrub tundra; (D) woodland (treeline analogue); (E) white spruce forest.

2.2. The study sites

Five different vegetation types were selected for study across a sequence of sites from tundra to mature white spruce (*Picea glauca*) forest (Fig. 2). The five sites were termed tundra, low shrub, tall shrub, woodland (treeline) and forest. These sites were located within 6 km radius of Council. This region of tundra and forest is representative of the contrast in vegetation that occurs across northern treeline (Lafleur, 1992). The cover of shrubs increased from tundra to woodland, but decreased substantially with the formation of a dense spruce overstory; trees were present only in the woodland and forest sites (Table 1; (Thompson et al., 2004)). The tundra site was a moist fruiticose-lichen, dwarf-shrub tundra that was dominated by low deciduous shrubs (mainly *Vaccinium uliginosum*), mosses and lichens (Walker et al., 1995). The low shrub site featured a moist low shrub tundra with deciduous shrubs, evergreen shrubs, and graminoid species in the understory; a ground cover of mosses was present. The tall shrub site was a moist shrub tundra dominated by tall deciduous shrubs (>1.5 m height) and low deciduous shrubs with a moss groundcover. The woodland site was a moist tall-shrub woodland and featured a spruce density of less than 100 trees ha⁻¹ and an average spruce height of 7.3 m (± 1.3 S.E.). Low deciduous shrubs, and graminoids dominated the understory with minimal moss groundcover. The forest site was a moist evergreen forest with a white spruce density of approximately 1100 trees ha⁻¹ and an average height of 6.1 m (± 0.3 S.E.) with a shrub understory and moss groundcover. The main functional groups, excluding spruce trees, and their cover values were derived from pindrop measurements at each site (Table 1). These cover values describe the functional group at the top of the canopy and tend to under-represent ground cover functional types such as mosses and lichens. Projected (single sided) leaf area index (LAI) was measured in these sites at the time of maximum aboveground biomass, using optical techniques with no additional corrections (Licor Inc., model LAI-2000). LAI varied across the sites from 0.52 at the tundra to 2.76 at the forest (Table 1; Fig. 3). More details on the vegetation and site characteristics can be found in Thompson et al., (2004). A description of soil properties and hydrologic characteristics on the Seward Peninsula can be found in Hofle et al. (1998).

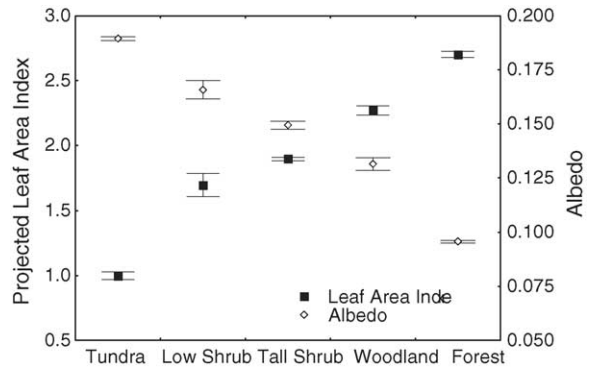


Fig. 3. Projected leaf area index and albedo for the major vegetation types across the vegetation gradient between tundra and forest. Mean and standard error bars are shown.

2.3. Surface energy exchanges

Three flux towers were deployed to characterize the radiation, energy and trace gas exchange simultaneously above the different vegetation types (McFadden et al., 1998). Two towers operated continuously during most of the growing season (6/18/99 to 8/22/99) at the forest and tundra sites, which represent the end members of the idealized vegetation gradient. A third tower was mobile and collected measurements consecutively at the woodland, low shrub, and tall shrub sites. The tundra tower was used as a reference tower to compare with the various mobile sites and the forest site because it had the most complete data set and represented an end member of the vegetation transition. Comparisons were made between the reference and mobile towers in a method developed by Eugster et al. (1997). We used 10 m towers at all sites except the forest site, where the tower was 20 m tall. The time system used here is local Alaskan Daylight Time (ADT), which is UTC–8 h. Throughout this paper the term daily refers to the 24-h period from midnight to midnight and daytime refers to the period when net radiation is positive (07:00–23:00). The term midday represents the 2 h either side of solar noon (13:00–17:00). Observations of energy and moisture exchange were made in conjunction with vegetation biomass and structure, soil thermal characteristics, permafrost characteristics, and parameters important in catchment-scale hydrological processes (Thompson et al., 2004).

Table 1

Details of site characteristics, radiation balance, surface energy exchanges, meteorological conditions, and structural properties of the five major vegetation types (Tundra, Low shrub, Shrub, Woodland and Forest) at Council, Seward Peninsula

	Tundra	Low shrub	Shrub	Woodland	Forest
Time period	18/6/99–22/8/99	14/7/99–27/7/99	4/8/99–22/8/99	19/6/99–13/7/99	18/6/99–22/8/99
Location	64° 50.499'N 163° 41.591'W	64° 53.47'N 163° 38.61'W	64° 56.141'N 164° 44.142'W	64° 53.997'N 163° 39.863'W	64° 54.456'N 163° 40.469'W
Vegetation					
Mosses (%)	10	1	2	3	8
Lichens (%)	18	3	0	0	0
Graminoids (%)	12	10	3	4	7
Forbs (%)	5	4	2	2	4
LD shrubs (%)	30	68	14	3	18
LE shrubs (%)	25	13	2	0	24
TD shrubs (%)	0	1	77	88	39
Site slope (°)	0	9	6	5	3
Site aspect (°TN)	0	236	160	140	140
Site elevation (m)	49	83	137	55	83
K_{down} (W m^{-2})	167 ± 3.6	146 ± 6.8	136 ± 5.9	268 ± 8.0	150 ± 3.8
K_{up} (W m^{-2})	33 ± 0.7	23 ± 6.1	18 ± 4.4	40 ± 7.6	14 ± 0.4
L_{down} (W m^{-2})	321 ± 0.5	325 ± 1.0	321 ± 0.9	312 ± 0.9	322 ± 0.5
L_{up} (W m^{-2})	362 ± 0.7	372 ± 1.7	359 ± 1.6	379 ± 2.1	354 ± 0.5
R_n (W m^{-2})	99 ± 2.6	83 ± 4.4	80 ± 4.0	158 ± 5.7	109 ± 3.1
R_n/K_{down}	0.59	0.57	0.59	0.59	0.73
Air temperature (°C)	11.4 ± 0.1	9.0 ± 0.1	10.5 ± 0.1	13.3 ± 0.2	11.5 ± 0.1
Soil bulk density (g cm^{-3})	0.14	0.31	0.29	0.33	0.24
Soil moisture volume (% at 10cm depth)	8.5 ± 0.06	21.4 ± 0.2	13.3 ± 0.05	38.7 ± 0.2	16.3 ± 0.04
VPD (mb)	5.2 ± 0.1	2.7 ± 0.3	2.5 ± 0.1	4.8 ± 0.3	3.9 ± 0.1
Wind speed at sonic height (m s^{-1})	1.7 ± 0.04	2.8 ± 0.07	1.4 ± 0.05	1.7 ± 0.03	1.4 ± 0.03
Albedo midday	0.19 ± 0.02	0.17 ± 0.003	0.15 ± 0.002	0.13 ± 0.002	0.10 ± 0.001
LAI at peak biomass	0.52	1.7	1.89	2.27	2.76
Bowen ratio daily (H/LE)	0.94	0.98	1.06	1.15	1.22
LE/R_n daily	0.36	0.35	0.36	0.36	0.37
H/R_n daily	0.34	0.35	0.38	0.41	0.44
G/R_n daily	0.12	0.12	0.08	0.10	0.05
$\Delta Q/R_n$ daytime	0.18	0.19	0.20	0.14	0.15
LE maximum (W m^{-2})	240	153	361	248	309
H maximum (W m^{-2})	316	268	288	335	404
G maximum (W m^{-2})	184	80	63	69	184
Omega midday	0.21 ± 0.004	0.28 ± 0.01	0.17 ± 0.006	0.15 ± 0.007	0.18 ± 0.005
Daily LE/LE_{eq}	0.55	0.61	0.61	0.59	0.42
Canopy height (m)	0.10	0.25	1.5	1.7 (shrubs), 7.3 (spruce)	6.1
Displacement height (m)	0.06	0.15	0.9	1.1	3.7
Roughness length (m)	0.04	0.08	0.18	0.74	1.6
Sonic height (m)	2.1	2.0	3.7	6.5	11.2
Available fetch (m)	1700	300	1000	500	1100
Aerodynamic resistance midday R_a (s m^{-1})	43 ± 2.6	20.8 ± 1.6	24.3 ± 3.1	13.1 ± 1.2	11.2 ± 0.9
Bulk surface resistance midday R_c (s m^{-1})	175 ± 10.9	170 ± 35.9	172 ± 11.1	146 ± 14.7	169 ± 24.0

Means and other statistical information were derived from the 30 min values over the measurement period. Note that the tundra and forest sites operated throughout the growing season whilst the other sites were measured sequentially using a single tower. Vegetation descriptions, summarized from Thompson et al. (2004), are percent cover of upper canopy functional groups except the forest where spruce trees are not included. Abbreviations are LD = low deciduous, LE = low evergreen and TD = tall deciduous.

2.4. Radiation balance

Radiation balance measurements were made at each site as close as practical to the top of the towers to minimize potential shading from above and to maximize the surface area within the effective sensor footprint (Schmid, 1997). Incoming and reflected shortwave as well as incoming and emitted long-wave radiation were measured using a pair of pyranometers (Eppley Labs Inc., model PSP) and pyrgeometers (Eppley Labs Inc., model PIR), respectively. An independent estimate of net radiation (R_n) above each surface was made using a Frischen-type net radiometer (REBS, model Q*7.1) with a wind-speed-dependant dome cooling correction applied to the results (REBS, March 1995).

2.5. Soil heat flux

Ground heat flux (G) was estimated via the combination method (Fuchs and Tanner, 1968) using heat flux plates (REBS, model HFT3) placed 10 cm below the surface in the organic mat and soil temperature measurements (REBS, model PRT) integrated over the top 10 cm above the heat flux plates. Ground heat flux measurements were made at four representative microclimate types per site (e.g. lichen-dominated versus moss-dominated microsites). Ground heat fluxes for each tower site were estimated using the area-weighted average of ground heat fluxes measured in each of the representative microsite types sampled (McFadden et al., 1998).

2.6. Convective fluxes (sensible and latent heat)

Eddy-covariance measurements were used to measure the convective fluxes of sensible (H) and latent heat (LE), as well as CO_2 fluxes. Measurements were made at different heights above the canopy depending on the underlying vegetation (shown as the sonic height in Table 1). Three dimensional wind velocities were measured using a 3D ultrasonic anemometer (Gill Solent, model HS) and were co-ordinate rotated (McMillen, 1988). Turbulent fluctuations of CO_2 and H_2O were measured using a closed path infrared gas analyzer (Licor, model LI-6262). The CO_2 and H_2O time series were lagged against the sonic temperature series to achieve the maximum correlation between the two time

series. Scalar quantities were linearly detrended and bell-tapered (Rannik and Vesala, 1999; Stull, 1988). A 3 mm internal diameter “Bev-A-Line” intake tube was used for the gas analyzer with an aspiration rate of approximately 7 L min^{-1} that ensured turbulent flow in the sample line (Lenschow and Raupach, 1991). In addition, 1.5 m of insulated copper tubing was placed inline to minimize temperature-induced density fluctuations (Leuning and Judd, 1996). The observations were logged at 10 Hz to a nearby laptop computer. Power was provided by a 2 kW generator located 100 m downwind from the tower.

The w‘T’ cospectra for each site followed the idealized cospectra (Kaimal et al., 1972). The w‘ CO_2 ’ and w‘ H_2O ’ were cospectrally corrected following Eugster and Senn (1995). Cospectral correction factors for water vapor were less than 1.4 during daylight hours. The energy balance closure ($\Delta Q/R_n$) was between 14 and 20% as a fraction of net radiation during the daylight hours (Table 1), where ΔQ is the energy balance residual. This indicated satisfactory measurement techniques and confidence in the measured fluxes (Eugster et al., 1997). In addition, the fetch was homogeneous and greater than 1 km in all directions at every site except the lowshrub and woodland sites, where the fetch was around 300 and 500 m, respectively. The slope and aspect along with the periods of measurement at each site is given in Table 1. High frequency eddy covariance data were despiked by removing data ± 3 S.D. from the 10-min mean for each scalar of interest. The 30-min averages were quality checked and data points ± 2 S.D. from the measurement period mean were removed. Data were screened to remove data where the wind direction was within a 45° section coming from behind the tower. No data gap filling was performed.

Climatic variables were measured every 30-s and 10-min averages were recorded on a data-logger (Campbell Scientific Inc., model CR10X). The mean temperature, wind speed, vapor pressure deficit, and soil moisture for the observation periods along with the soil bulk density for each site are given in Table 1. Profiles of air temperature and water vapor content above and below the level of the sonic anemometer were measured using temperature/relative humidity probes (Vaisala, model HMP45C). Wind speed at the radiometer height was measured using a cup anemometer (R.M. Young, model 03101).

2.7. Calculations

For each site we calculated the equilibrium evaporation rate LE_{eq} , which represents the lower limit to evaporation from moist surfaces (Jarvis and McNaughton, 1986). We calculated aerodynamic resistance for momentum transfer (R_a) ($s\ m^{-1}$) following (Kelliher et al., 1995). Bulk surface resistance (R_c) ($s\ m^{-1}$)

determined using eddy covariance measurements and an inversion of the following Penman–Monteith equation following (Wallace, 1995). We examined the coupling of the surface to the atmosphere by calculating an Omega value (decoupling co-efficient) for each site, according to Jarvis and McNaughton (1986).

Observed fluxes were measured using the eddy covariance towers (Fig. 4) but are not all directly

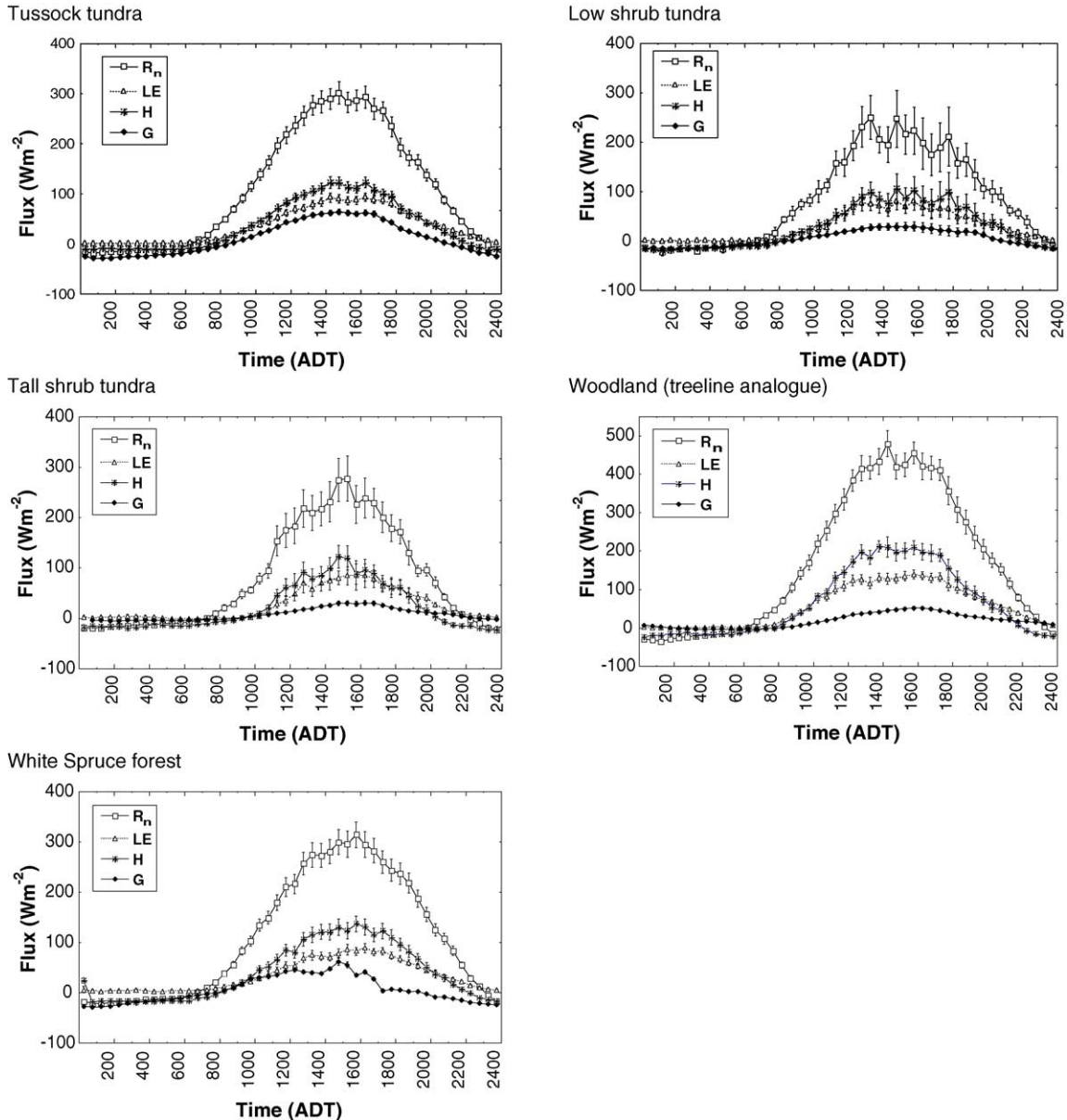


Fig. 4. Mean diurnal surface energy exchange plots for the period of measurement at each site with standard error bars shown.

comparable among sites because insolation (and hence R_n) changes over the different periods of measurement among the mobile sites. We reduce the confounding influence of variation in R_n among different periods of measurement across sites by comparing the partitioning of energy at the surface using ratios of H , LE and G to R_n at the surface for the measurement period at each site (Table 1; Fig. 5). In addition, we utilize a common climatic index called the Bowen ratio (H/LE) (Bowen, 1926).

The meteorological and surface conditions can vary across the course of a growing season, which will impact on the resultant fluxes to the atmosphere. Such changes have been well documented by Rouse et al. (1987) and Lafleur and Rouse (1988), in the Arctic for example. In our study, seasonal changes were evident in the changing Bowen ratio at the tundra site (0.90–1.03) during different periods of measurement associated with the different deployment times of

the mobile tower (Fig. 5). Similar variability was seen at the forest site and probably occurred across the mobile sites. To help account for these potential seasonal differences we normalized the energy balance ratios to the reference site (tundra) to account for temporal differences between sites (Fig. 6). The data can then be interpreted as a fractional difference between data gathered simultaneously at the mobile and tundra sites (Fig. 6). Values of greater than one indicate higher ratios at the mobile site compared to the tundra site and vice versa.

It should be noted that although the seasonal changes can be minimized by comparing normalized values we cannot account for all the changes across the season. In particular phenological changes such as leaf out will alter energy partitioning. We attempted to minimize this by measuring only during the established growing season. The exception is the woodland site where leaf out was occurring and the snow had just

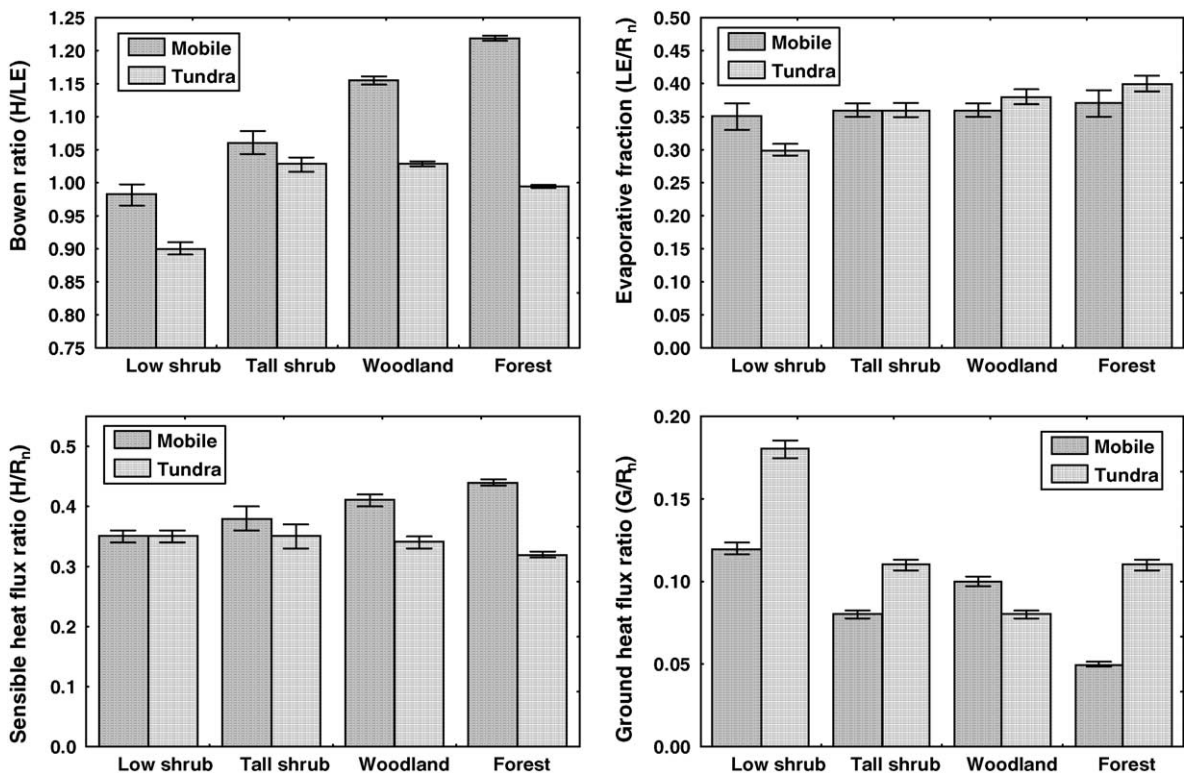


Fig. 5. The Bowen ratio, evaporative fraction, sensible heat flux ratio and ground heat flux ratio for each of the mobile sites (low shrub, tall shrub, woodland and forest). Adjacent bars show the simultaneous ratios of energy partitioning from the tundra site (reference) for the same period of measurement as the mobile site. Mean and standard error bars are shown.

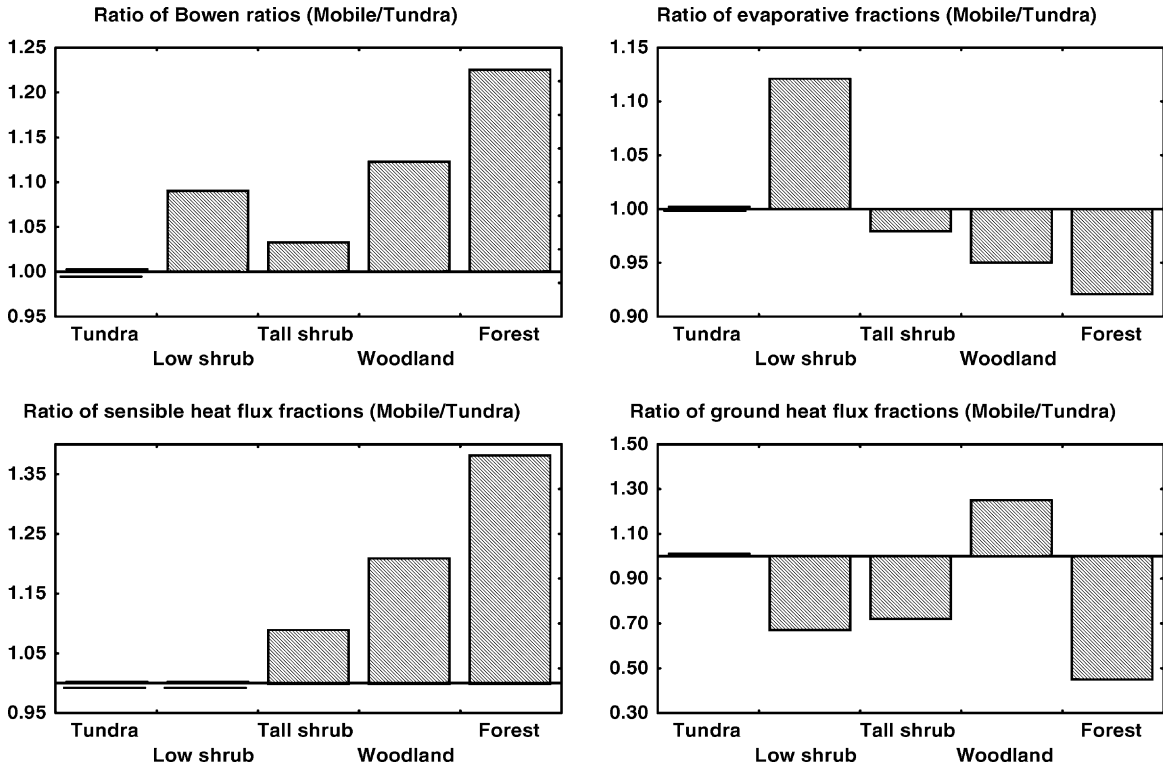


Fig. 6. Fractions of the energy partitioning ratios for the tundra vs. the other sites (low shrub, tall shrub, woodland and forest). This removes seasonal variations in climate between the sites by comparing the ratios to a reference site (tundra). Values above 1 indicate that the ratio was greater than the tundra for the same time period. Values below 1 indicate that the ratio was less than the tundra for the same time period. Mean and standard error bars are shown.

melted allowing free evaporation to occur and a relatively low bulk surface resistance (R_c) (Table 1). We used the later part of that data to reduce the effect but could not eliminate it and this highlights one of the problems in trying to compare data from mobile towers across a season.

3. Results and discussion

3.1. Radiation balance

Average July incoming shortwave radiation (K_{down}) across sites was around 150 W m^{-2} , which is slightly lower than the 200 W m^{-2} found for other arctic sites near this latitude (Eugster et al., 2000). This is likely a result of frequent maritime cloudiness after mid-summer in the Seward Peninsula region. Differences in R_n among sites are due to differences in K_{down} over

the measurement period along with the site-specific albedo ($\alpha = K_{\text{up}}/K_{\text{down}}$) and the net longwave radiation ($L^* = L_{\text{down}} - L_{\text{up}}$), where L_{down} is the incoming longwave radiation, L_{up} is the outgoing longwave radiation and K_{up} is the reflected shortwave radiation from the surface. Albedo and L^* could both vary with phenology over the course of a season and therefore, because measurements at the mobile tower sites were taken at different times of the season we cannot directly compare among the mobile sites. The net radiation showed less hourly variation for the sites measured during the early summer period when conditions were clear (woodland) (Fig. 4). For sites measured over the entire season (tundra and forest) the large sample size also results in a small standard error (Fig. 4).

Comparing the relative radiation components minimizes the confounding influences of differences in measurement date on R_n . In our study we assume

that K_{down} was similar at any point in time across the sites because they were all within 6 km of each other. The ratio of net radiation at the surface over incoming shortwave radiation (R_n/K_{down}) is a function of surface albedo and the longwave balance and was relatively constant around 0.6 across sites in our transition, except for the forest site where the ratio was 0.73 (Table 1). This indicates that, for a given shortwave input, the forest site would have a 20% larger net radiation than the other sites. This increased energy would then be available for partitioning into sensible, latent and ground heat fluxes. Therefore, any difference in energy partitioning at the forest is likely to be amplified because of the greater amount of net radiative energy available at the surface.

The ratio of $L_{\text{up}}/L_{\text{down}}$ was similar (1.10–1.14) across all sites except the woodland site (1.21), where clear skies in the early summer resulted in higher surface temperatures and increased L_{up} along with lower sky temperatures and lower L_{down} (Table 1). In our sites, the magnitude of R_n was dominated by net shortwave (K^*) rather than net longwave (L^*), and therefore the site differences in R_n were controlled primarily by differences in albedo and variations in K^* rather than L^* .

Albedo decreased nearly 50% across the transition from tundra (0.19) to forest (0.10) (Table 1; Fig. 3). Albedos calculated in this study were consistent with values of 0.19–0.16 for tundra (Eugster et al., 2000; Fitzjarrald and Moore, 1992), 0.15–0.16 for shrub tundra (Eugster et al., 1997; McFadden et al., 1998) and 0.11 for black spruce forest (Jarvis et al., 1997; Pattey et al., 1997). Our measurement of tundra albedo of 0.19 was on the higher side of other measured values, most likely as a result of the high lichen cover at the site. The decline in albedo along the gradient was due to spectral and structural differences in vegetation primarily driven by differences in the composition and distribution of plant functional types (Table 1). Spectral differences include decreasing abundance of reflective surfaces (lichens and standing dead from graminoids). The structural differences from tundra to forest include increasing LAI (Table 1) that increases the radiation trapping efficiency of the canopy (Oke, 1987) and masks the relatively reflective understory of lichens and mosses. Increased LAI combined with increased canopy height and biomass increases the complexity of the canopy, which in turn decreases albedos (Fig. 3).

3.2. Surface energy exchanges

The energy exchanges at the surface drive local climate through input of heat and water to the atmosphere. Hence, any differences in the energy partitioning among sites could lead to distinctly different local climates. We present the seasonally averaged surface energy balance for each vegetation type across the transition for each respective measurement period (Fig. 4). Midday H was slightly dominant over LE at all sites, so the midday Bowen ratio was greater than one. At most sites the maximum LE occurred later than the peak in H , and in the late afternoon LE tended to be greater than H (Fig. 4). This delay may be due to a peak in air temperature and vapor pressure deficit (VPD) that both occur after the peak in R_n and H . In a well-coupled system such as ours the later peak in VPD drives LE higher at this time also. After midnight LE was near zero, but there was a transfer of heat from the soil and atmosphere toward the surface that is expressed by small negative fluxes of H and G (Fig. 4). The measured magnitudes are not directly comparable so flux ratios have been used for further analysis.

3.3. Soil heat flux

The fraction of net radiation conducted into the soil (G/R_n) varied from 0.05 to 0.12 for the forest and tundra, respectively (Table 1). The difference in G/R_n among sites probably results from site differences in canopy shading, with the forest (and to a lesser extent tall shrub and woodland) having less radiation at the ground surface and therefore less ground heat flux than the tundra or low shrub. Permafrost, which was found only at the tundra site, could also have contributed to the large tundra ground heat flux by creating a strong thermal gradient between the ground surface and depth. This may have offset the influence of the highly insulative moss cover in the tundra site which would otherwise have been expected to reduce soil heat flux (Beringer et al., 2001a). This pattern is consistent with observations in the Canadian sub-Arctic (Boudreau and Rouse, 1995; Lafleur et al., 1997; Rouse, 1984b) and the Arctic, where forest tundra had 6% of R_n partitioned into G (McFadden et al., 1998). The daily ratio G/R_n was greater than typical mid-latitude sites where G/R_n approaches zero, because of the long day

lengths at higher latitudes in summer (Stull, 1988) and strong thermal gradients from the surface to the cold underlying soils.

3.4. Latent heat flux (LE)

The amount of energy used in latent heating (LE) is otherwise known as evapotranspiration (ET) and consists of both transpiration and evaporation components. The evaporative fraction ($EF = LE/R_n$) varied only slightly among all sites, ranging from 0.35 to 0.37 (Table 1). In previous studies of arctic vegetation types on the North Slope of the Brooks Range during the LAII-FLUX study (Kane and Reeburgh, 1998), the EF increased twofold from the driest heath site (0.21) to wettest moist sedge site (0.42) (McFadden et al., 1998). However, the range of EF values for sites with equivalent vegetation to ours (tussock tundra, tussock-shrub and shrub tundra) was 0.35–0.38, consistent with our observations.

Although the measured EF was similar across sites, these sites were measured at different times. A comparison of the EF of the mobile sites with the equivalent period at the tundra (reference) site showed that the EF at the tundra site increased slightly over time between the different measurement periods (Fig. 5). Hence all the EF's must be normalized to the reference tower. When this is done, a comparison of the EF among the mobile sites showed that they were within approximately 10% of the tundra site (Fig. 6). However, the EF tended to be slightly lower at the tall shrub, woodland and forest sites relative to the tundra (Fig. 6). This indicates that for equivalent periods, there were relatively greater latent heat fluxes at the tundra and low shrub sites, which are likely a result of the sparse canopy cover and relatively unrestricted evaporation of moisture from the moist unshaded moss surface.

Soil moisture has been considered an important factor in controlling LE between vegetation types in the Arctic. For instance, (McFadden et al. (1998) found a strong relationship between actual and equilibrium LE (LE_{eq}) and volumetric soil water content across a heath to shrub tundra gradient on the North Slope of Alaska. Lafleur et al. (1992) found that soil moisture was the most important factor in controlling site differences between tundra and open forest in Canada. However, in our study there was no clear relationship

between soil moisture and LE across different vegetation types. In addition, there was no clear correlation between average daily soil moisture and average daily LE within a vegetation type, for any of the sites (forest $r = -0.06$, $n = 54$, $p > 0.05$; woodland $r = -0.09$, $n = 20$, $p > 0.05$; tall shrub $r = 0.35$, $n = 19$, $p > 0.05$; low shrub $r = -0.08$, $n = 8$, $p > 0.05$; tundra $r = -0.27$, $n = 56$, $p > 0.05$). The lack of correlation may occur in our tundra and low shrub sites because of the relatively high soil water content that allows free evaporation from the soil and mosses almost all of the time. The poor correlation at the tall shrub, woodland and forest sites may occur because the ground surface is isolated from the atmosphere. This lack of correlation within a site is consistent with results from the North Slope of Alaska (McFadden et al., 1998).

Despite the lack of correlation between LE and soil water content, there appeared to be a distinct shift in the contributions of evaporation and transpiration to LE. At the sites with little or no canopy cover (tundra and low shrub), soil and moss evaporation presumably dominates LE. At sites with a well-developed canopy (shrub, woodland and forest), transpiration contributes the most significant fraction. This is evident from sap flow measurements taken at the spruce forest site during our study, which indicate that transpiration was the major contributor (77%) to LE (Wendt, 2001). In a synthesis of conifer stands, Baldocchi et al. (2000) found that across spruce forest sites between 50 and 62% of LE comes from transpiration. Transpiration is in turn partly controlled by stomatal and boundary resistances to water vapor transport which are in turn related to atmospheric conditions (Oke, 1987). Moisture in the soil will therefore support transpiration but result in only a small forest floor evaporation because of the shading from the overstorey canopy. Although we expect the evaporation from the floor to be controlled by radiation, the contribution to total LE is small, resulting in the total LE at our forest site being dominated by transpiration and overall better correlated with VPD rather than R_n . Although we found no relationship between soil moisture and LE, we did find significant linear relationships of increasing average daily LE with increasing VPD across all sites (forest $r = 0.580$, $n = 54$, $p < 0.05$; woodland $r = 0.336$, $n = 20$, $p < 0.05$; tall shrub $r = 0.571$, $n = 19$, $p < 0.05$; low shrub $r = 0.693$, $n = 8$, $p < 0.05$; tundra $r = 0.841$, $n = 56$, $p < 0.05$).

These relationships are typical of ecosystems that are well coupled to the atmosphere because the bulk air directly influences transpiration from the vegetation through VPD and changes in surface resistance (Kelliher et al., 1995). In our study, the tall shrub, woodland and forest sites had omega values between 0.15 and 0.18 suggesting that these sites were well coupled to the atmosphere (Table 1). This is consistent with higher LAI and a dominance of transpiration to LE, which is partly stomataly controlled. At the tundra and low shrub sites, the canopy was not well developed and hence soil and mosses, which have no stomatal control over water loss, evaporated more freely (Beringer et al., 2001a). Therefore the tundra and low shrub tundra sites had slightly higher omega values (0.21–0.28, respectively) indicating that they were less well coupled to the atmosphere (Table 1). However, the correlation between VPD and LE was strongest at the tundra and decreased along the transition to the forest. At our tundra site the average VPD for the period of measurement was higher in the tundra than the forest by 20% (Table 1) and therefore may help drive a better correlation with VPD. At the forest site where VPD was lower the stomatal resistance was not as sensitive to VPD and was not as well correlated. We also calculated the correlation for LE/R_n and found that the correlation coefficients were lower than for VPD/R_n and that the correlation was greatest in the tundra and decreased along the transition to shrub and forest (forest $r = 0.276$, $n = 54$, $p < 0.05$; woodland $r = 0.060$, $n = 20$, $p > 0.05$; tall shrub $r = 0.360$, $n = 19$, $p < 0.05$; low shrub $r = 0.080$, $n = 8$, $p > 0.05$; tundra $r = 0.430$, $n = 56$, $p < 0.05$). This suggests that R_n is more important in driving LE at the tundra site than at the shrub or forest, most likely because the tundra site is energy limited. This is also consistent with Baldocchi et al. (2000) who suggest that ET is generally weakly coupled to R_n in conifer stands. Nevertheless, all sites were more tightly coupled to the atmosphere than grassland, crops and other short-statured ecosystems where omega is typically 0.5–0.9 (Jarvis and McNaughton, 1986).

The relationship between VPD and LE along with small omega values and low LE/LE_{eq} ratios (Table 1) suggests that total ET was driven to a large extent by atmospheric conditions such as the drying power of the air (VPD). These bulk atmospheric conditions are in turn determined to a large degree by synoptic-scale

weather features (Rouse, 1984a). Across our transition from tundra to forest, we suggest the increasing LAI served to shade the surface and limit soil evaporation but conversely increase transpiration. The net result was that LE was conserved but the sources changed. As the sources change to become increasingly dominated by transpiration, the controls over LE will also change. We suggest that the synoptic scale atmospheric influences such as VPD are important drivers of LE from arctic vegetation at our sites at Council. Further, this suggests that warming-induced increases in leaf area and biomass of arctic vegetation, as observed across our tundra to forest transition, could alter the sources and controls of LE, making water loss more sensitive to synoptic-scale controls over VPD.

3.5. Canopy structure and resistance

The latent heat flux from the surface is partly controlled by the aerodynamic and bulk surface resistances to water vapor transport that in turn determine how strongly an ecosystem is coupled to the atmosphere (omega). Vegetation structure itself controls the aerodynamic resistance (R_a) to transport of water vapor with smooth surfaces having a higher resistance. Structural parameters such as canopy height (h) and roughness length (Z_o) impact aerodynamic resistance and have been identified in land surface model sensitivity analyses as important parameters for determining fluxes (Beringer and Tapper, 2002). In our study, canopy height increased from 0.1 to 6.1 m across the gradient from tundra to forest, as shrub and needleleaf evergreen plant functional types became dominant. The corresponding increase in roughness length from 0.04 to 1.6 m is important in determining r_a and this decreased from 43 to 11.2 $s\ m^{-1}$ from tundra to forest. Across our sites LAI was an excellent predictor for Z_o and the aerodynamic drag co-efficient (C_D) ($\log - Z_o = -4.55 + 1.70LAI$, $r^2 = 0.8558$, $t = 4.212$, $n = 5$, $p < 0.05$ and $C_D = 0.0291 + 0.0478LAI$, $r^2 = 0.838$, $t = -0.390$, $n = 5$, $p < 0.05$ and). Z_o was better correlated with LAI than canopy height due to the difficulty in assigning a canopy height to the woodland site, which had scattered spruce trees. Our study demonstrates why structural parameters, such as LAI, are important to land surface and climate models.

3.6. Sensible heat flux and Bowen ratio

It is notable that the EF was almost constant between the tundra and forest sites, and omega was relatively small (<0.3) over all the sites (but higher in the tundra and low shrub sites). However, the sensible heat fraction (H/R_n) increased almost 35% from 0.34 to 0.44 across the transition (Table 1; Fig. 5). Similarly, there was a trend of increasing sensible heat fraction relative to the tundra site along the sequence (Fig. 6). This indicates that a greater proportion of energy is used in heating the atmosphere across the sequence from tundra to forest. This is reflected in the Bowen ratio that increased across the vegetation sequence from the low leaf tundra (0.94) to the high leaf forest (1.22) (Table 1; Fig. 5). Our Bowen ratios are consistent with other studies, for example, tundra Bowen ratios of 0.4–1.0 (Eugster et al., 2000) and 1.01 (McFadden et al., 1998) have been reported. Bowen ratios for black spruce forest of 1.04 (Den Hartog et al., 1994) and 1.35–1.90 (Pattey et al., 1997) have been documented.

The large increase in sensible heat fraction from tundra to forest and the relative constancy of the EF across sites (Table 1) suggests that these two turbulent fluxes are controlled by different factors. Both fluxes are sensitive to aerodynamic resistance (R_a) (coupling of the surface to the atmosphere) and surface temperature, but EF also depends on bulk surface resistance to water vapor (R_c) flux from the surface. Both EF and R_c are relatively constant across sites (Table 1). Across the transition we hypothesize that at the tundra site, where the LAI is low, the surface moss layer can desiccate rapidly and provide the primary resistance to water loss. LAI increases across the gradient to forest which results in increased shading and higher R_c . This effectively reduces soil/moss evaporation as LAI increases across the gradient, but simultaneously increases transpiration from the leafy canopy. As leaf area increases, stomata become the primary source of resistance. Hence although R_c is conserved, the sources of that resistance as well as the sources of ET change as LAI increases. The outcome is that if climatic warming in the Arctic causes a shift of vegetation from tundra to forest, then there is likely to be (1) an increase in LAI and canopy complexity, (2) a decrease in G due to increased shading of the soil by the canopy, (3) a decrease in albedo, (4) a much

greater available energy for partitioning into H and LE , (5) higher Bowen ratios. This subsequently results in a significant increase in atmospheric heating as vegetation transitions from tundra to forest and could impact local to regional climate.

3.7. Seasonal flux comparisons between vegetation types

Energy exchange ratios are useful but do not, by themselves, determine the magnitudes of the fluxes among sites. Moreover, even measured differences in K^* and L^* between sites are not comparable because K_{down} and L_{down} change through the growing season (Table 1). In order to determine the effect of surface properties on the magnitudes of surface energy fluxes, we developed a simple empirical model that used the radiation and energy balance ratios at each site to construct the surface energy exchanges for a given input of shortwave and longwave radiation. We estimated K^* and L^* for each site by taking the mean K_{down} and mean L_{down} from the tundra site during the growing season (Table 1) and applying these mean values to each site, using the site-specific shortwave and longwave albedos. The result is an R_n calculated for each site that has been normalized to K_{down} and L_{down} at the tundra site (Fig. 7). Given this estimate of R_n , we can then use the ratio of G/R_n as well as the Bowen ratio (H/LE) to construct the convective (H and LE) and conductive (G) fluxes for each site (Fig. 7), which can be more directly compared.

The estimates from the constructed energy balances show the magnitudes of average growing season fluxes at each site normalized to the tundra site (Fig. 7; Table 2). With warming in the Arctic, we expect a shift along the transition from tundra to forest through the intermediate vegetation types (Kittel et al., 2000). Our results indicate that the surface energy exchanges do not change linearly along this transition despite a relatively linear change in LAI and albedos. Rather we found non-linear responses with the largest shifts in energy exchanges occurring from low shrub to shrub and from shrub to woodland. The dramatic change in surface energy exchanges between low shrub and tall shrub resulted from the development of a full leafy canopy ($LAI \sim 1$), which shaded the soil and provided a change in the sources of ET and R_c . Contrary to our expectations, there was a greater change in energy

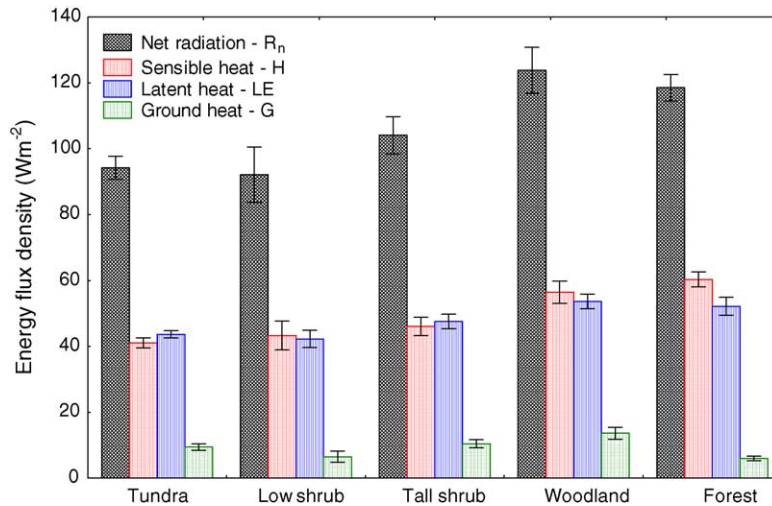


Fig. 7. Composite daily mean surface energy exchanges for each site. Net radiation from all sites except the tundra were composed using the short and long wave albedos from each site and applying these to the mean incoming short and long wave radiation from the tundra site during the growing season. The convective and conductive fluxes were composed from the net radiation and the ratios of G/R_n and the Bowen ratio (H/LE) at each site. In order to indicate measurement error in the fluxes we have included the standard error (S.E.) of the observed flux measurements.

exchange between tall shrub and woodland than between woodland and forest. The reason for this is uncertain; however, it is evident that the major changes in energy balance occur across the tundra to tall shrub and the tall shrub to forest transitions. These transitions have already been identified as having important feedbacks to climate (Beringer et al., 2001b; Chapin et al., 2000b), and we have determined the mean surface energy exchange differences resulting from transitions among the major vegetation types (Table 2). Our results indicate that a shift from tundra to tall shrub would result in an increase of 9.9 W m^{-2} in R_n and a 7.1 and 1.8 W m^{-2} increase in H and LE , respectively. In addition, G would increase by 1.0 W m^{-2} . A change from tall shrub tundra to forest would result in an increase of 14.4 W m^{-2} in R_n and a 13.7 and 5.2 W m^{-2} increase in H and LE , respectively (Table 2). This increase in turbulent fluxes associated with the addition of trees is much larger than would be expected from the increase in LAI (Fig. 3), suggesting that the unique structure of spruce trees contributes disproportionately to roughness length and therefore the efficiency of convective exchange. The more discrete nature of roughness elements in a spruce forest compared to a relatively continuous shrub canopy may contribute to the effectiveness of spruce trees in promoting convective

exchange. In addition, G would decrease by 4.5 W m^{-2} in the spruce forest. These large changes in daily average fluxes represent the local radiative forcing associated with each vegetation change. The climatic consequences of these transitions between vegetation types were also considered in a regional modeling study over Alaska that examined the differences in forcing that were driven by predefined differences in land surface properties such as albedo, roughness length, displacement height and leaf and stem area indices (Chapin et al., 2000b). Our direct observations of fluxes are consistent with their study (Table 2), in that the magnitude of change from shrub to forest is greater than from tundra to shrub. However, the magnitudes of our changes are two to three times greater. The lower magnitudes simulated by Chapin et al. (2000a) are due mainly to the smaller changes in albedo between vegetation types that they used to parameterize their model runs in comparison to our observed data (Table 2).

Of the convective fluxes, sensible heating has a direct effect on local and regional climate through heating of the boundary layer and is of primary interest (Oke, 1987). Our results suggest that a vegetation transition from tundra to tall shrub and then to forest will result in increases in sensible heating of 7.1 and 13.7 W m^{-2} , respectively. Increased sensible heating

Table 2
The mean growing season albedo and energy exchanges for each site at Council

	Albedo	R_n (W m^{-2})	H (W m^{-2})	LE (W m^{-2})	G (W m^{-2})
Tundra	0.19	94.2	41.1	43.7	9.4
Low shrub	0.17	92.1	42.4	43.2	6.4
Shrub	0.15	104.1	48.2	45.5	10.4
Woodland	0.13	123.8	58.9	51.2	13.6
Forest	0.10	118.5	61.9	50.7	5.9
Tundra to low shrub	−0.02	−2.1	1.3	−0.5	−3
Low shrub to shrub	−0.02	12	5.8	2.3	4
Shrub to woodland	−0.02	19.7	10.7	5.7	3.2
Woodland to forest	−0.03	−5.3	3	−0.5	−7.7
Tundra to shrub	−0.04	9.9	7.1	1.8	1.0
Shrub to forest	−0.05	14.4	13.7	5.3	−4.5
Tundra to shrub ^a	−0.005	0.9	3.4	2.2	−1.1
Shrub to forest ^a	−0.025	4.6	4.5	−9.0	−10.0

Also given are the magnitudes of changes in albedo and the energy balance components resulting from a change in vegetation type across the transition. Values for the tundra to tall shrub and tall shrub to forest are calculated and compared with previously modeled values.

^a Chapin et al. (2000a).

is significant in the context of other forcings on climate such as a doubling of CO_2 that is calculated to result in a global radiative forcing at the top of the troposphere (IPCC, 2001). The influence of large-scale vegetation changes on warming is also large compared to the shift from glacial to interglacial during the Pleistocene, where a 2% change in solar constant resulted in an equivalent change in radiative forcing of 1 W m^{-2} (IPCC, 2001).

It should be noted that increased sensible heating observed in our study results in local- to regional-scale warming of the boundary layer. The amount of heating also depends on the area of vegetation converted, and its direct effect is largely restricted to the area where the vegetation change occurs. In contrast, any effects due to a doubling of CO_2 are global due to the rapid mixing of greenhouse gases in the atmosphere, an effect that lasts throughout the year. The effect of increased heating from these vegetation transitions could be enhanced, as arctic growing seasons lengthen (Zhou et al., 2001). Even in winter, a vegetation change to tall shrubs and subsequently to forest is also likely to increase sensible heating (especially in spring when sun angles are high) due to a masking of snow by an emergent plant canopy that reduces surface albedo (Bonan et al., 1992; Foley et al., 1994) and the reduction in ground heat flux due to more insulative snow cover in shrub- and forest-dominated sites (Sturm et al., 2001).

The timescales on which the two major vegetation transitions occur are also distinctly different, with a change from tundra to tall shrub occurring on the order of decades (Chapin et al., 1995; Silapaswan, 2000; Sturm et al., 2001), whereas a transition from tall shrub to forest occurs on the order of centuries (Starfield and Chapin, 1996). This distinction is important because enhanced warming can result in an increase in shrubs on relatively short timescales. This suggests that a positive biotic feedback between increasing shrubbiness and warming could be very rapid and that a transition from tundra to forest need not occur in order to see strong feedbacks to climate. Finally, the net effect of these transitions will also depend on changes in carbon storage (e.g. (Betts, 2000)) in these ecosystems and is an area that needs further research.

4. Conclusions

Changes in energy balance characteristics that we measured over a vegetation transition from tundra to forest were directly related to structural parameters of the canopy such as leaf area, canopy height, and canopy complexity. The Bowen ratio increased from the tundra to forest sites, indicating an increasing dominance of H as the primary energy source to the atmosphere. This effect is amplified by the increase in

R_n as the structure of the canopy becomes more complex and albedo decreases. Increased LAI, together with increased canopy height, and changes in the distribution of canopy elements, augments the multiple scattering and absorption of radiation, leading to a lower albedo. These structural changes resulted in large changes in surface energy exchange across our vegetation sequence. As LAI increased, the shading of the ground may have strongly inhibited direct soil evaporation but transpiration may have increased. This results in the moisture transfer to the atmosphere being more strongly controlled by larger scale meteorological parameters such as VPD than by local soil moisture. The role of seasonality, including the spring and fall transitions, in controlling surface energy partitioning remains an important topic for further research.

We conclude that a transition of vegetation from tundra to tall shrub and then to forest could result in increased H during the growing season on the order of 7.1 and 13.7 W m^{-2} , respectively. Even though the tall shrub site had an intermediate LAI between the tundra and forest, the change in H was not intermediate between the two; instead the greatest change in H occurred between tall shrub and forest. This illustrates that there may be non-linear changes in surface energy exchanges along a gradient of increasing LAI and that other structural and physiological parameters may be important. We suggest that transitions in vegetation that result from climate warming will result in a positive feedback to further warming in the Arctic. Based on our research in these transitional ecosystems, this biotic feedback to increased warming may be greater than previously thought (Chapin et al., 2000b) and is regionally significant in the context of other forcings on climate such as a doubling of CO_2 .

Acknowledgements

Thanks to Dr. D.A. Walker for vegetation descriptions for the sites, the participants in the Research Experience for Undergraduates for field assistance. We would like to thank Dr. Michaela Dommissie for her comments on the manuscript and Dr. Peter Lafleur and an anonymous reviewer for their constructive reviews. This research is supported through the Arctic

System Science (ARCSS) program of the National Science Foundation (OPP-9732126).

References

- Baldocchi, D.D., Kelliher, F.M., Black, T.A., Jarvis, P., 2000. Climate and vegetation controls on boreal zone energy exchange. *Global Change Biol.* 6 (Suppl. 1), 69–83.
- Beringer, J., Lynch, A.H., Chapin, F.S., Mack, M., Bonan, G.B., 2001a. The representation of arctic soils in the land surface model: the importance of mosses. *J. Climate* 14 (15), 3324–3335.
- Beringer, J., Tapper, N., 2002. Surface energy exchanges and interactions with thunderstorms during the maritime continent thunderstorm experiment (MCTEX). *J. Geophys. Res.-Atmos.* 107 (D21), 4552–4552.
- Beringer, J., Tapper, N., McHugh, I., Chapin III, F.S., Lynch, A., Serreze, M.C., Slater, A.G., 2001b. Impact of Arctic treeline on synoptic climate. *Geophys. Res. Lett.* 28 (22), 4247–4250.
- Betts, R.A., 2000. Offset of the potential carbon sink from boreal forestation by decreases in surface albedo. *Nature* 408 (6809), 187–190.
- Bonan, G.B., Chapin, F.S., Thompson, S.L., 1995. Boreal forest and tundra ecosystems as components of the climate system. *Climatic Change* 29, 145–167.
- Bonan, G.B., Pollard, D., Thompson, S.L., 1992. Effects of boreal forest vegetation on global climate. *Nature* 359, 716–718.
- Boudreau, L.D., Rouse, W.R., 1995. The role of individual terrain units in the water balance of wetland tundra. *Climate Res.* 5, 31–47.
- Bowen, I.S., 1926. The ratio of heat losses by conduction and by evaporation from any water surface. *Phys. Rev.* 27, 779–787.
- Bret-Harte, M.S., Shaver, G.R., Zoerner, J.P., Johnstone, J.F., Wagner, J.L., Chavez, A.S., Gunkelman, R.F., Lippert, S.C., Laundre, J.A., 2001. Developmental plasticity allows *Betula nana* to dominate tundra subjected to an altered environment. *Ecology* 82 (1), 18–32.
- Chapin, F.S., Eugster, W., McFadden, J.P., Lynch, A.H., Walker, D.A., 2000a. Summer differences among Arctic ecosystems in regional climate forcing. *J. Climate* 13 2002–1602.
- Chapin, F.S., McGuire, A.D., Randerson, J., Pielke Sr., R., Baldocchi, D., Hobbie, S.E., Roulet, N., Eugster, W., Kasischke, E., Rastetter, E.B., Zimov, S.A., Running, S.W., 2000b. Arctic and boreal ecosystems of western North America as components of the climate system. *Global Change Biol* 53 (Suppl. 1), 211–223.
- Chapin, F.S., Shaver, G.R., Giblin, A.E., Nadelhoffer, K.J., Laundre, J.A., 1995. Responses of arctic tundra to experimental and observed changes in climate. *Ecology* 76 (3), 694–711.
- Ciais, P., Tans, P.P., Trolier, W., White, J.W.C., Francey, R.J., 1995. A large northern hemisphere terrestrial CO_2 sink indicated by the $^{13}\text{C}/^{12}\text{C}$ ratio of atmospheric CO_2 . *Nature* 269 (5227), 1098–1102.
- Den Hartog, G., Neumann, H.H., King, K.M., Chipanshi, A.C., 1994. Energy budget measurements using eddy correlation and Bowen ratio techniques at the Kinosheo Lake tower during the

- Northern Wetlands Study. *J. Geophys. Res-Atmos.* 99 (d1), 1539–1549.
- Eugster, W., McFadden, J.P., Chapin, F.S., 1997. A comparative approach to regional variation in surface fluxes using mobile eddy correlation towers. *Boundary-Layer Meteorol.* 85, 293–307.
- Eugster, W., Rouse, W., Pielke Sr., R.A., McFadden, J.P., Baldocchi, D., Kittel, D., Chapin III, T.G.F., Liston, F.S., Vidale, G.E., Vaganov, P.L., Chambers, E.S., 2000. Land-atmosphere energy exchange in Arctic tundra and boreal forest: available data and feedbacks to climate. *Global Change Biol.* 6 (Suppl. 1), 84–115.
- Eugster, W., Senn, W., 1995. A cospectral correction model for measurement of turbulent NO₂ flux. *Boundary-Layer Meteorol.* 74, 321–340.
- Fitzjarrald, D.R., Moore, K.E., 1992. Turbulent transport over tundra. *J. Geophys. Res-Atmos.* 97 (D15), 16717–16729.
- Fleming, M.D., Chapin III, F.S., Cramer, W., Hufford, G.L., Serreze, M.C., 2000. Geographic patterns and dynamics of Alaskan climate interpolated from a sparse station record. *Global Change Biol.* 6 (Suppl. 1), 49–58.
- Foley, J.A., Kutzbach, J.E., Coe, M.T., Levis, S., 1994. Feedbacks between climate and boreal forests during the Holocene epoch. *Nature* 371, 52–54.
- Fuchs, M., Tanner, C.B., 1968. Calibration and field test of soil heat flux plates. *Soil Sci. Soc. Am. Proc.* 32, 326–328.
- Hobbie, S.E., Shevtsova, A., Chapin, F.S., 1999. Plant responses to species removal and experimental warming in Alaskan tussock tundra. *Oikos* 84 (3), 417–434.
- Hofle, C., Ping, C.-L., Kimble, J.M., 1998. Properties of permafrost soils on the northern Seward Peninsula, Northwest Alaska. *Soil Sci. Soc. Am. J.* 62 (6), 1629–1639.
- IPCC, 2001. *Climate Change 2001: The Scientific Basis. Contribution of Working Group I to the Third Assessment Report of the Intergovernmental Panel on Climate Change.* Cambridge University Press, Cambridge, United Kingdom and New York, NY, USA, 881 pp.
- Jarvis, P.G., Masseder, J.M., Hale, S.E., Moncrieff, J.B., Rayment, M., Scott, S.L., 1997. Seasonal variation of carbon dioxide, water vapour and energy exchanges of a boreal black spruce forest. *J. Geophys. Res-Atmos.* 102, 28953–28966.
- Jarvis, P.G., McNaughton, K.G., 1986. Stomatal control of transpiration: scaling up from leaf to region. *Adv. Ecol. Res.* 15, 1–47.
- Kaimal, J.C., Wyngaard, J.C., Izumi, Y., Cote, O.R., 1972. Spectral characteristics of surface-layer turbulence. *Q. J. Roy. Meteor. Soc.* 98, 563–589.
- Kane, D.L., Reeburgh, W.S., 1998. Introduction to special section: land-air-ice interactions (LAI) flux study. *J. Geophys. Res-Atmos.* 103 (D22), 28913–28915.
- Kelliher, F.M., Leuning, R., Raupach, M.R., Schulze, E.D., 1995. Maximum conductances for evaporation from global vegetation types. *Agric. For. Meteorol.* 73 (1–2), 1–16.
- Kittel, T.G.F., Steffen, W.L., Chapin III, F.S., 2000. Global and regional modelling of Arctic-boreal vegetation distribution and its sensitivity to altered forcing. *Global Change Biol.* 6 (Suppl. 1), 1–18.
- Lafleur, P.M., 1992. Energy balance and evapotranspiration from a subarctic forest. *Agric. For. Meteorol.* 58, 163–175.
- Lafleur, P.M., McCaughey, J.H., Joiner, D.W., Bartlett, P.A., Jelinski, D.E., 1997. Seasonal trends in energy, water, and carbon dioxide fluxes at a northern boreal wetland. *J. Geophys. Res-Atmos.* 102, 29009–29020.
- Lafleur, P.M., Rouse, W., 1988. The influence of surface cover and climate on energy partitioning and evaporation in a subarctic wetland. *Boundary-Layer Meteorol.* 44, 327–347.
- Lafleur, P.M., Rouse, W.R., Carlson, D.W., 1992. Energy balance differences and hydrologic impacts across the northern treeline. *Int. J. Climatol.* 12, 193–203.
- Lenschow, D.H., Raupach, M.R., 1991. The attenuation of fluctuations in scalar concentrations through sampling tubes. *J. Geophys. Res-Atmos.* 96 (D8), 15259–15268.
- Leuning, R., Judd, M.J., 1996. The relative merits of open- and closed-path analysers for measurement of eddy fluxes. *Global Change Biol.* 2, 241–253.
- Levis, S., Foley, J.A., Pollard, D., 1999. Potential high-latitude vegetation feedbacks on CO₂-induced climate change. *Geophys. Res. Lett.* 26 (6), 747–750.
- MacDonald, G.M., Velichko, A.A., Kremenetski, V., Borisova, O.K., Goleva, A.A., Andreev, A.A., Cwynar, L.C., Riding, R.T., Forman, S.L., Edwards, T.W.D., Aravena, R., Hammarlund, D., Szeicz, J.M., Gattaulin, V.N., 2000. Holocene treeline history and climate change across northern Eurasia. *Quart. Res.* 53, 302–311.
- McFadden, J.P., Chapin, F.S., Hollinger, D.Y., 1998. Subgrid-scale variability in the surface energy balance of arctic tundra. *J. Geophys. Res.* 103 (D22), 28,947–28,961.
- McGuire, A.D., Klein-Curley, J.S., Melillo, J.M., Kicklighter, D.W., Meier, R.A., Vorosmarty, C.J., Serreze, M.C., 2000. Modelling carbon responses of tundra ecosystems to historical and projected climate: sensitivity of pan-Arctic carbon storage to temporal and spatial variation in climate. *Global Change Biol.* 6 (Suppl. 1), 141–159.
- McMillen, R.T., 1988. An eddy correlation technique with extended applicability to non-simple terrain. *Boundary-Layer Meteorol.* 43, 231–245.
- Nickels, S., Furgal, C., Castleden, J., Moss-Davies, P., Buell, M., Armstrong, B., Dillon, D., Fonger, R., 2002. Putting the human face on climate change through community workshops. In: Krupnik, I., Jolly, D. (Eds.), *The Earth is Faster Now: Indigenous Observations of Arctic Environmental Change.* Arctic Research Consortium of the United States, Fairbanks, USA, pp. 300–333.
- Oke, T.R., 1987. *Boundary Layer Climates.* Routledge, London, pp. 435.
- Pattey, E., Desjardins, R.L., St. Armour, G., 1997. Mass and energy exchange over a black spruce forest during key periods of BOREAS. *J. Geophys. Res-Atmos.* 102, 28967–28975.
- Rannik, U., Vesala, T., 1999. Autoregressive filtering versus linear detrending in estimation of fluxes by the eddy covariance method. *Boundary-Layer Meteorol.* 91 (2), 259–280.
- REBS, March 1995. *Radiation and Energy Balance Systems Q*7.1 Net Radiometer Manual.* Radiation and Energy Balance Systems, Seattle, WA.

- Reeburgh, W.S., Whalen, S.C., 1992. High latitude ecosystems as CH₄ sources. *Ecol. Bull.* 42, 62–70.
- Rouse, W.R., 1984a. Microclimate at arctic tree line 3. The effects of regional advection on the surface energy balance of upland tundra. *Water Resour. Res.* 20 (1), 74–78.
- Rouse, W.R., 1984b. Microclimate of Arctic tree line 2. Soil microclimate of Tundra and forest. *Water Resour. Res.* 20 (1), 67–73.
- Rouse, W.R., Hardill, S.G., Lafleur, P., 1987. The energy balance in the coastal environment of James Bay and Hudson Bay during the growing season. *J. Climatol.* 7, 165–179.
- Schmid, H.P., 1997. Experimental design for flux measurements: matching scales of observations and fluxes. *Agric. For. Meteorol.* 87, 179–200.
- Silapaswan, C., 2000. Land cover change on the Seward Peninsula: The use of remote sensing to evaluate the potential influences of climate change on historical vegetation dynamics, University of Alaska Fairbanks, Fairbanks.
- Starfield, A.M., Chapin, F.S., 1996. Model of transient changes in Arctic and Boreal vegetation in response to climate and land use change. *Ecol. Appl.* 6 (3), 842–864.
- Stull, R.B., 1988. An introduction to boundary layer meteorology. Kluwer Academic Publications, Dordrecht, Holland, pp. 670.
- Sturm, M., Racine, C., Tape, K., 2001. Increasing shrub abundance in the Arctic. *Nature* 411, 546–547.
- Thompson, C., Beringer, J., Chapin, F.S., McGuire, A.D., 2004. Structural complexity and land-surface energy exchange along a gradient from arctic tundra to boreal forest. *J. Veg. Sci.* 15, 397–406.
- Thorpe, N., Eyegetok, S., Hakongak, N., Elders, K., 2002. Nowadays it is not the same: inuit Quajimajatuqangit, climate and caribou in the Kitikmeot Region of Nunavut, Canada. In: Krupnik, I., Jolly, D. (Eds.), *The Earth is Faster Now: Indigenous Observations of Arctic Environmental Change*. Arctic Research Consortium of the United States, Fairbanks, USA, pp. 198–239.
- Walker, D.A., Auerbach, N.A., Lewis, B.E., Shippert, M.M., 1995. NDVI, biomass, and landscape evolution of glaciated terrain in northern Alaska. *Polar Rec.* 31, 169–178.
- Wallace, J.S., 1995. Calculating evaporation—resistance to factors. *Agric. For. Meteorol.* 73 (3–4), 353–366.
- Wendt, C., 2001. Controls over evapotranspiration in an arctic boreal White Spruce forest, Monash University, Melbourne.
- Zhou, L.M., Tucker, C.J., Kaufmann, R.K., Slayback, D., Shabanov, N.V., Myneni, R.B., 2001. Variations in northern vegetation activity inferred from satellite data of vegetation index during 1981 to 1999. *J. Geophys. Res.-Atmos.* 106 (D17), 20069–20083.